REPORT DOCUMENTATION PAGE

Form Approved
OMB NO. 0704-0188

1. AGENCY USE ONLY (Leave Blank)	2. REPORT DATE	3. REPORT TYPE AND DATES COVERED

4. TITLE AND SUBTITLE
New Features of Scattering from a Dielectric Film on a Reflecting Metal Substrate (part 1)

5. FUNDING NUMBERS
DAAD19-02-C-0056

6. AUTHOR(S)

Zu-Han Gu, I.M. Fuks, Mikael Ciftan

7. PERFORMING ORGANIZATION NAME(S) AND ADDRESS(ES)

Surface Optics Corp
11555 Rancho Bernardo Road
San Diego, CA 92127

8. PERFORMING ORGANIZATION REPORT NUMBER

9. SPONSORING / MONITORING AGENCY NAME(S) AND ADDRESS(ES)

U. S. Army Research Office
P.O. Box 12211
Research Triangle Park, NC 27709-2211

10. SPONSORING / MONITORING AGENCY REPORT NUMBER

42991.8 - PH

11. SUPPLEMENTARY NOTES

The views, opinions and/or findings contained in this report are those of the author(s) and should not be construed as an official Department of the Army position, policy or decision, unless so designated by other documentation.

12 a. DISTRIBUTION / AVAILABILITY STATEMENT

Approved for public release; distribution unlimited.

12 b. DISTRIBUTION CODE

13. ABSTRACT (Maximum 200 words)

See Attached

14. SUBJECT TERMS

15. NUMBER OF PAGES

16. PRICE CODE

17. SECURITY CLASSIFICATION OR REPORT	18. SECURITY CLASSIFICATION ON THIS PAGE	19. SECURITY CLASSIFICATION OF ABSTRACT	20. LIMITATION OF ABSTRACT
UNCLASSIFIED	**UNCLASSIFIED**	**UNCLASSIFIED**	**UL**

Wave Propagation, Scattering and Emission in Complex Media
Edited by Ya-Qiu Jin
Science Press and World Scientific, 2004

New Features of Scattering from a Dielectric Film on a Reflecting Metal Substrate* (Part I)

Zu-Han Gu[1], I.M.Fuks[2], Mikael Ciftan[3]

[1]Surface Optics Corporation
11555 Rancho Bernardo Road, San Diego, CA, 92127-1441, USA

[2] Zel Technologies, LLC and NOAA/ETL, 325 Broadway, Boulder, CO, 80305-3328, USA

[3]U.S. Army Research Office, P.O. Box 12211, Research Triangle Park, NC, 27709, USA

Abstract

We have recently observed several features from a randomly rough dielectric film on a reflecting metal substrate including the change in the spectrum of the light at the satellite peaks, the high order correlation and enhanced backscattering from the grazing angle. In this paper we will focus on the enhanced backscattering phenomena.

The backscattering signal at small grazing angles is very important for vehicle re-entrance and subsurface radar sensing applications. Recently, we performed an experimental study of the far-field scattering at small grazing angles, especially the enhanced backscattering at grazing angles. For a randomly weak rough dielectric film on a reflecting metal substrate, a much larger enhanced backscattering peak is measured. Experimental results are compared with the theoretical predictions based on the two-scale surface roughness scattering model.

Keywords: *Enhanced backscattering effect, coherence effect, rough surface scattering.*

1. Introduction

Interference effects with diffuse light have been studied for a long time. A recorded observation of the phenomenon was made by Newton about three centuries ago,(1) with a description of the appearance of a series of colored rings when a beam of sunlight falls on a concave, dusty back-silvered spherical mirror. The phenomenon was explained later by Young(2) and Herschel by considering the interference between two streams of light: one scattered on entering the glass and the other scattered on emerging from the glass.

For scattering of light from a rough dielectric film on a reflecting substrate, there are three main kinds of trajectories that give rise to (a) Quetelet fringes, (b) Selenyi fringes, and (c) enhanced backscattering. A typical Quetelet ring pattern consists of a series of elongated colored diffuse rings. The white ring, corresponding to the zero order of interference, passes through both the

* Correspondence: E-mail: zgu@surfaceoptics.com; Telephone: (858) 675-7404; FAX: (858) 675-2028.

specular and the backscattering directions, and as the angle of incidence is changed, new colors emerge from the center.

Besides the Quetelet-type ring, there is another kind of interference effect that has been observed in the scattering of light from dusty, backsilvered mirrors. The Selenyi rings[3] present a different kind of behavior under oblique illumination; there is no zero-order ring, and the rings are always centered about the normal to the sample. The occurrence of such rings has been explained in terms of the interference between waves scattered back directly from the top of the scattering layer without entering it, and waves reflected by the mirror after first having been scattered when entering the film.

One of the most interesting phenomena associated with the scattering of light from a randomly rough surface is that of enhanced backscattering. This is the presence of a well-defined peak in the retroreflection direction in the angular distribution of the intensity of the incoherent component of the light scattered from such a surface. It results primarily from the coherent interference of each multiply reflected optical ray with its time-reversed partner.

The scattering of light from a one-dimensional randomly rough dielectric film deposited on a flat reflecting substrate is studied.[4-5] In particular, the appearance of well-defined fringes in the angular distribution of the diffusely scattered intensity and their dependence on the angle of incidence, the roughness of the film, and the film's mean thickness is investigated. It is found that, for slightly rough films, the angle of incidence modulates the intensity of the fringes but has no effect on their angular position. For rougher films the contrast of the pattern decreases, and the fringes move with the angle of incidence in such a way that there are always bright fringes in the specular and backscattering directions. Eventually, for very rough films, the fringe pattern disappears, and a well-defined backscattering peak emerges in the retroreflection direction.

The measurement of the scattering of electromagnetic waves from a randomly rough surface at grazing angles of incidence presents a challenging problem.[6] This is due at least in part by the fact that if, say, a one-dimensional random surface is illuminated by a beam of finite width W, see Figure 1, its intercept with the mean scattering surface $\Delta = W/\cos(\theta_i)$, where θ_i is the angle of incidence measured counter clockwise from the normal to the mean scattering plane, increase to a very large value as θ_i approaches 90°. For example, if $\theta_i = 89°$, $\Delta = 57.3\ W$. We have to select a small beam size W about 1.5 mm and sample length L of the random surface should be large enough to compromise the grazing angle edge effect. L is chosen to be 200 mm.

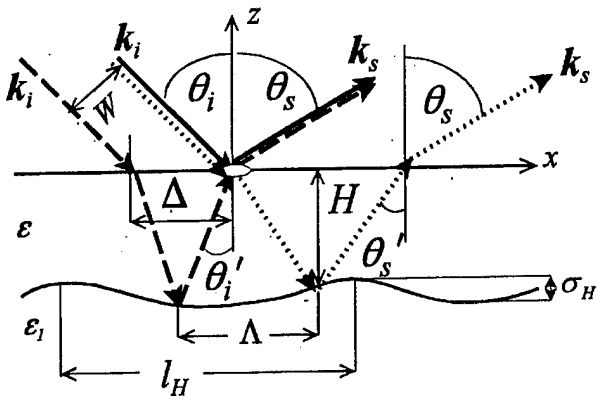

Figure 1. **Physical schematic with indicatrix scattering.**

In this paper, we report the observation of enhanced backscattering at grazing angle. Part 2 will introduce the theoretical analysis followed by Part 3, the experimental results, and Part 4, the summary.

2. *Theoretical Analysis*

Theoretical analysis of electromagnetic wave scattering from a randomly rough boundary of an arbitrary plane layered medium was performed in [7] and [8] by employing the small perturbation method. It was assumed that the surface roughness height $\varsigma(\mathbf{r})$ (where $\mathbf{r} = \{x, y\}$ is a radius-vector in the plane $z = 0$ of the medium boundary) is much smaller than the incident wave length λ.

The specific (referred to the unit area of surface $z = 0$) scattering cross-section $\sigma^0_{\alpha\beta}(\mathbf{k}_s, \mathbf{k}_i)$ of plane incident wave with wave vector $\mathbf{k}_i$ (see Fig.1) and polarization state $\beta = p, s$ [s polarization corresponds to the direction of electric vector is perpendicular to the plane of incidence xOz, and p polarization corresponds to electrical vector lies in this plane] into the scattered plane wave with the wave vector $\mathbf{k}_s = (k_0 \sin\theta_s \cos\varphi_s, k_0 \sin\theta_s \sin\varphi_s, k_0 \cos\theta_s)$ and the polarization state $\alpha = p,s$ [s polarization corresponds to electrical vector is perpendicular to the plane of scattering, that form the azimuthal angle φ with the plane of incidence xOz, and p polarization corresponds to electrical vector lies in this plane] can be written in the following form (see Eq.(5.3) in [8]):

$$\sigma^0_{\alpha\beta}(\mathbf{k}_s, \mathbf{k}_i) = \pi k_0^4 |\varepsilon - 1|^2 \left| f_{\alpha\beta} \right|^2 S_\varsigma(\mathbf{q}_\perp) \tag{1}$$

where $k_0 = 2\pi / \lambda$ is the wave number, $\varepsilon \equiv \varepsilon(0)$ is the upper limit value of the dielectric permittivity $\varepsilon(z)$ in the medium (z<0), $\mathbf{q} = \mathbf{k}_s - \mathbf{k}_i$ is a "vector of scattering", $\mathbf{q}_\perp$ is its projection on the plane z=0, and $S_\varsigma(\mathbf{q}_\perp)$ is a spatial power spectrum of surface roughness which can be introduced as a Fourier transformation of roughness auto-correlation function $W(\rho) = \overline{\varsigma(r+\rho)\varsigma(\rho)}$:

$$S_\varsigma(\mathbf{p}) = \frac{1}{(2\pi)^2} \iint W(\rho) e^{ip\rho} d\rho, \tag{2}$$

where the bar $\overline{\ldots}$ denote the statistical averaging over ensemble of random function $\varsigma(\mathbf{r})$, and factors $f_{\alpha\beta}$ (that are proportional to the ``amplitude" or ``length" of scattering) are given by the expressions (5.6) - (5.9) from [8]:

$$f_{ss} = [1 + R_s(\theta_i)][1 + R_s(\theta_s)] \cos\varphi \tag{3}$$

$$f_{ps} = -[1 - R_p(\theta_s)][1 + R_s(\theta_i)] \cos\theta_s \sin\varphi \tag{4}$$

$$f_{pp} = \frac{1}{\varepsilon}\left[1+R_p(\theta_i)\right]\left[1+R_p(\theta_s)\right]\sin\theta_i \sin\theta_s - \\ -\left[1-R_p(\theta_i)\right]\left[1-R_p(\theta_s)\right]\cos\theta_i \cos\theta_s \cos\varphi \tag{5}$$

$$f_{sp} = \left[1-R_p(\theta_i)\right]\left[1+R_s(\theta_s)\right]\cos\theta_i \sin\varphi \tag{6}$$

Here R_s and R_p are the specular reflection coefficients from the lower ($z<0$) stratified media into the upper half-space ($z>0$) for s and p polarizations, correspondingly.

In a particular case of uniform (homogeneous) media with $\varepsilon(z) = \varepsilon = Const.$, when there is no volume scattering at all in the half-space $z<0$, coefficients R_p and R_s coincide with the usual Fresnel reflection coefficients R_{0p} and R_{0s} from the plane interface of two homogeneous media ($\varepsilon_0 = 1$, $z>0$) and (ε, $z>0$):

$$R_{op} = \frac{\varepsilon\cos\theta - \sqrt{\varepsilon - \sin^2\theta}}{\varepsilon\cos\theta + \sqrt{\varepsilon - \sin^2\theta}}; \qquad R_{os} = \frac{\cos\theta - \sqrt{\varepsilon - \sin^2\theta}}{\cos\theta + \sqrt{\varepsilon - \sin^2\theta}}. \tag{7}$$

In a general case of an arbitrary stratified media the reflection coefficients R_p and R_s can be represented in a form:

$$R_{p,s} = \frac{R_{0p,s} + R'_{p,s}}{1 + R_{0p,s}R'_{p,s}} \tag{8}$$

where $R'_{p,s}$ are the reflection coefficients from the buried layers ($R'_{p,s} = 0$ for the uniform $\varepsilon(z) = Const.$ homogeneous half-space $z<0$).

Here we apply this general theory to the simplest case of layered structure: the homogeneous dielectric layer of thickness H and permittivity ε lying on the homogeneous half-space ($z \le H$) with a complex dielectric permittivity constant ε_1. The reflection coefficient $R_{p,s}(\theta)$ from this structure for every linear polarization (s,p) is given by the Equation (8), where $R'_{p,s}(\theta)$ can be written in the form $R'_{p,s}(\theta) = R_{1p,s}(\theta)\exp[i\varphi(\theta)]$, where $R_{1p,s}(\theta)$ is the Fresnel reflection coefficient from the interface of two media with dielectric permittivity constants ε and ε_1:

$$R_{1s} = \frac{\sqrt{\varepsilon - \sin^2\theta} - \sqrt{\varepsilon_1 - \sin^2\theta}}{\sqrt{\varepsilon - \sin^2\theta} + \sqrt{\varepsilon_1 - \sin^2\theta}}; \; R_{1p} = \frac{\varepsilon_1\sqrt{\varepsilon - \sin^2\theta} - \varepsilon\sqrt{\varepsilon_1 - \sin^2\theta}}{\varepsilon_1\sqrt{\varepsilon - \sin^2\theta} + \varepsilon\sqrt{\varepsilon_1 - \sin^2\theta}}. \tag{9}$$

and $\varphi(\theta) = 2k_0 H\sqrt{\varepsilon - \sin^2\theta}$.

The detailed analysis of the intensity spatial distribution pattern, originated from scattered by roughness $z = \varsigma(\mathbf{r})$ and multiple reflected (from planes $z=0$ and $z=-H$) wave interference, was done in [8]: the interference rings angular positions, their polarization dependence, periods of intensity oscillations as functions of parameters H and λ etc. These theoretical results are in a good

agreement with experiments carried out with the perfect Fabry-Perot parallel-slided plates ($H = Const.$) and the very small surface settled scatterers (see, e.g., [9]). But in some experiments (see [10]) an essential disagreement with this theory was discovered. In [10] it was shown that the large-scaled roughness (LSR) can be the main reason of destroying the interference between some type of waves, that leads to the "surviving" only the one specific set of interference maxima and suppressing the others. The theoretical analysis conducted in [10] was restricted to consideration of interference of once reflected waves only. For very low grazing angle of incidence $\pi/2-\theta_i$ the multiple wave reflections into the resonator formed by two planes $z=0$ and $z=-H$ can play the leading role in forming the scattered field intensity spatial distribution, and in particular, in forming the backscattering intensity peak

To investigate the effect of the LSR on the scattered intensity distribution, we assume that the successive wave reflections inside the layer ($0>z>-H$) every time take place from a horizontal plane (as it is depicted in Fig. 1) without changing the reflective angles θ_i' and θ_s' correspondingly before and after scattering by the rough patch of upper boundary), but the layer thickness H is different at the different points of reflection, as it shown in Fig. 1. The solution of this modeling problem can be represented in form (1) with amplitudes $f_{\alpha\beta}$, which can be obtained from those given by (3) through (6), with the following formal procedure. In $f_{\alpha\beta}$ representation by mentioned above equations, the factors $\left|1 \pm R_{s,p}\right|$ can be rewritten in the form, using (8):

$$1 \pm R = \frac{R_0 \pm 1}{R_0}\left[1 \pm \frac{R_0 \mp 1}{1 + R_0 R'}\right]. \tag{10}$$

Here, for short, we omit the arguments (θ_i and θ_s) or only their subscripts (i and s), and the polarization subscripts (p and s) in reflection coefficients, insomuch as it does not lead to confusion. Expand (10) in a series of $R' = R_1 \exp[i\varphi]$ powers, which is equivalent to field representation as a series of multiplicity reflection, we substitute instead $n\varphi$ the phase of the wave n-times reflected from the undulated interface between layer and substrate $n\varphi \Rightarrow \sum_{k=1}^{n}\phi_k$, where $\varphi_k(\theta) = 2k_0 H_k\sqrt{\varepsilon - \sin^2\theta}$, and $\{H_k\}$ is the set of layer thicknesses in the specular reflecting points:

$$1 \pm R \Rightarrow \frac{R_0 \pm 1}{R_0}\left[1 \pm (R_0 \mp 1)\sum_{n=0}^{\infty}(-R_0 R_1)^n \exp\left(i\sum_{k=1}^{n}\phi_k\right)\right]. \tag{11}$$

After this we can consider H as a random function of two variables (x,y), with a given average value $\langle H \rangle$, variance σ_H^2 and correlation length l_H.

Here we assume that there are no losses inside the dielectric layer, i.e., $\mathrm{Im}\,\varepsilon = 0$ and present results only for the limiting case of extremely strong variations of layer thickness σ_H^2, when the corresponding Rayleigh parameter essentially exceeds the unity, i.e.,

$$\left\langle (\delta\phi_k)^2 \right\rangle = 4k_0^2\sigma_H^2\left(\varepsilon - \sin^2\theta_s\right) = \left(2k_1\sigma_H \cos\theta_s'\right)^2 >> 1, \tag{12}$$

where θ_s' and θ_s are related by Snell's refraction law: $\sin\theta_s' = \sin\theta_s / n$, $n = \sqrt{\varepsilon}$ is a refraction index, and $k_1 = nk_0$. If this inequality holds, it is possible to neglect the averaged value of exponents in (11), i.e., take $\langle \exp(i\phi_k) \rangle = 0$ in all equations that appears from (11).

The result of statistical averaging of scattered light intensity angular distribution over the set of random variables $\{H_k\}$, which we denote by the corner brackets $\langle ... \rangle$, strongly depends on the ratio of correlation length l_H and the distances Λ between the sequential specular reflecting points (see Fig. 1). If all distances Λ between every two arbitrary reflecting points from the substrate exceed essentially the correlation length l_H, then all subsequent specular reflections from the lower layer boundary can be considered as independent random events, and consequently the set of ϕ_k is the set of independent variables. Thus if inequality $\Lambda >> l_H$ holds, then in all directions of scattering given by angles θ_s, φ, excluding the vicinity of backscattering direction ($\theta_s = \theta_i, \varphi = \pi$), the factors $1 \pm R(\theta_i)$ and $1 \pm R(\theta_s)$ are statistically independent and can be averaged separately. Statistical average value of the scattering cross section $\langle \sigma_{\alpha\beta}^0 \rangle$ over layer thickness fluctuations $\delta H = H - \langle H \rangle$ is proportional to the $\langle |f_{\alpha\beta}|^2 \rangle$, which for s polarization takes the form (see (3)):

$$\langle |f_{ss}|^2 \rangle = \langle |1 + R_s(\theta_i)|^2 \rangle \langle |1 + R_s(\theta_s)|^2 \rangle \cos^2\varphi \tag{13}$$

Compare the scattering cross section $\langle \sigma_{ss}^0 \rangle$, averaged over the layer thickness variations, with the corresponding value $\overline{\sigma}_{ss}$ for the homogeneous half-space bounded by the same rough surface. The explicit equation for $\overline{\sigma}_{ss}$ is given by (1) with f_{ss} from (3), where the reflection coefficients R_s have to be substituted by R_{0s}, i.e., if we put $R_s' = 0$ in all above equations. For ratio of these two cross-sections (which can be named, according to [11], as a contrast coefficient K_{ss}) we obtain:

$$K_{ss} = \frac{\langle \sigma_{ss}^0 \rangle}{\overline{\sigma}_{ss}} = C(\theta_i) C(\theta_s), \tag{14}$$

where function $C(\theta)$ is given by equation:

$$C(\theta) = \frac{1 + r_1^2 (1 + 2r_0)}{1 - (r_0 r_1)^2}, \tag{15}$$

here, $r_0 = |R_{0s}|$ and $r_1 = |R_{1s}|$. In a special case of perfectly conducting substrate when $r_1 = 1$, (15) takes the form:

$$C(\theta) = \frac{2}{1 - r_0(\theta)}, \tag{16}$$

and we obtain the simple equation for the contrast coefficient (14):

$$K_{ss}(\theta_s,\theta_i)=\frac{4}{(1-r_0(\theta_i))(1-r_0(\theta_s))}. \tag{17}$$

It follows from this equation that $K_{ss}(\theta_s,\theta_i)\geq 4$, because $0\leq r_0(\theta_{i,s})\leq 1$, and in a particular case of $\varepsilon >> 1$, when

$$1-r_0(\theta)=\frac{2\cos\theta}{\sqrt{\varepsilon-\sin^2\theta}+\cos\theta}\cong\frac{2\cos\theta}{\varepsilon}, \tag{18}$$

we obtain for $K_{ss}(\theta_s,\theta_i)$:

$$K_{ss}(\theta_s,\theta_i)=\frac{\varepsilon}{\cos\theta_s\cos\theta_i}>>1. \tag{19}$$

It is seen that the average brightness of interference pattern due to the substrate can essentially exceed the one for homogeneous half-space (without substrate) even for very strong variations of layer thickness δH when all the interference maxima are utterly smoothen.

The backscattering case has to be considered separately because the dashed and dotted ray trajectories in Figure 2 are fully congruent in this case, and it is impossible to carry out the averaging over δH separately for each of them. When $\theta_s=\theta_i$ and $\varphi=\pi$, and all specular reflecting points for dashed and dotted rays coincide, we have to carry out the following averaging:

$$\left\langle\sigma_{ss}^0\right\rangle\approx\left\langle\left|1+R_s(\theta_i)\right|^4\right\rangle, \tag{20}$$

where $1+R_s(\theta_i)$ is represented as a sum (11) of independent specular reflections from the undulated substrate.

Skipping over the bulky derivations we present here only the final expression for the contrast coefficient K_{0ss} in backscattering direction as a result of averaging in the limiting case of very strong layer thickness fluctuations δH, when the inequality (12) holds:

$$K_{0ss}=\frac{\left\langle\left|1+R_s\right|^4\right\rangle}{\left|1+R_{0s}\right|^4}=\left\{\left(1+r_1^2\right)\left[(1+r_1^2)(1+A)+8r_1^2r_0\right]+2r_1^2\left[(1-A)^2+2A(3-A)\right]\right\}(1-A)^{-3}, \tag{21}$$

where $A=(r_0r_1)^2$ and θ_i is supposed to be an argument for all reflection coefficients. Compare K_{0ss} given by (21) with the indicatrix contrast coefficient K_{ss} given by (14) for directions of scattering θ_s close to backscattering (i.e., putting there $\theta_s=\theta_i$ and $\mathbf{k}_s=-\mathbf{k}_i$, we can estimate the excess γ of backscattering peak of $\left\langle\sigma_{ss}^0(-\mathbf{k}_i,-\mathbf{k}_i)\right\rangle$ over the surrounding background:

$$\gamma = \frac{K_{0ss}}{K_{ss}}. \tag{22}$$

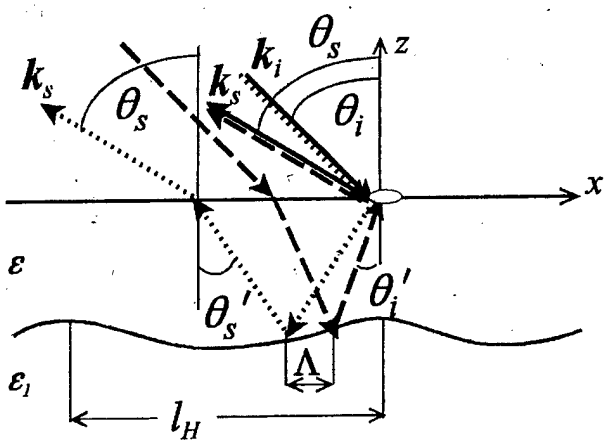

Figure 2. **Physical schematic for near backscattering direction.**

Equation (21) takes the simpler form for the specific case of perfectly conducting substrate when $r_1 = 1$:

$$K_{0ss} = \frac{2(3-r_0)}{(1-r_0)^3}. \tag{23}$$

Compare this expression with the indicatrix contrast coefficient K_{ss} given by (17) for directions of scattering θ_s close to backscattering (i.e., putting there $\theta_s = \theta_i$:

$$K_{ss} = \frac{4}{[1-r_0(\theta_i)]^4}, \tag{24}$$

we can estimate the excess γ of backscattering peak of $\left\langle \sigma_{ss}^0(-\mathbf{k}_i,-\mathbf{k}_i) \right\rangle$ over the surrounding background in this specific case :

$$\gamma = \frac{(3-r_0)}{2(1-r_0)}. \tag{25}$$

It is easy to see that the general phenomena of backscattering enhancement, in the specific problem under consideration, appears as a backscattering peak enhancement that for $(1-r_0) << 1$

can essentially (many times) exceed the background, in contrast to the well-known volume scattering problem, where this enhancement can achieve the value of several units only. In a specific case of low grazing angle or big layer dielectric permittivity ε, when inequality $\sqrt{\varepsilon - \sin^2\theta_i} >> \cos\theta_i$ holds, from (25) follows:

$$\gamma = \frac{\sqrt{\varepsilon - \sin^2\theta_i}}{2\cos\theta_i} >> 1. \tag{26}$$

It is worth to emphasize that all above equations for contrast coefficients K_{ss} and K_{0ss}, as well as for backscattering peak enhancement γ, do not depend on the statistical parameters of upper surface roughness, and in particular, on its spatial power spectrum $S_\varsigma(\mathbf{q}_\perp)$. For non-absorptive dielectric layer with $\mathrm{Im}\,\varepsilon = 0$ they do not depend also on the mean layer thickness $\langle H \rangle$ and its variance σ_H^2, if inequality (12) holds.

3. *Experimental Results*

A fully automated bidirectional reflectometer in Figure 3 is used to measure the fraction of incident light reflected by the sample into incremental angles over its field of view. It uses illumination from laser sources at 0.633 μm and enables measurements for any combination of incident and reflected angles over the entire plane, except for a small angle (about 0.5° away from the retroreflection direction) in which the source and detector mirrors interfere. A laser beam passes through a polarizer and is interrupted by a chopper and a half-wavelength plate, which enables rotation of the polarization of the beam. Then it is directed toward the sample by a folded beam system that collimates it into a parallel beam up to 25mm diameter. For the measurement, the beam size is set to 1.5 mm. The sample is viewed by a movable off-axis paraboloid that projects the light reflected by the sample onto the detector via a polarizer and a folding mirror. Four different polarization combinations of input and receiving beams are recorded. The reference standard used for these experiments is lab Sphere Gold, and the relative bidirectional reflectance is measured. The signal is recorded and digitized at each angular setting of interest throughout the angular range by an ITHACO lock-in amplifier and the data are stored in the memory of a personal computer (PC). The sample and the receiving telescope arm are separately mounted on two rotational stages run by two independent stepper motors that are controlled by the PC via a two-axis driver. Since the beam size is small, thus the average far-field speckle size is large. We have to average about 100 measurements to obtain the far-field scattering at each angle by scanning very small yaw and pitch directions of the sample.

The sample we used is a smooth aluminum that was coated with a dielectric film for high performance and protection. The thickness of the layer is approximately H = 5.2 μm. The complex permittivity ε_1 of Al at λ = 0.6328 μm is $\varepsilon_1 = -56.52+21.25i$. The refractive index of film is n = 1.64 (the dielectric constant is ε = 2.69). The rms height of the roughness of the film is about 60Å and 1/*e* correlation length is about 3000Å. The illuminating source in the experiment is a 15 mW He-Ne laser with λ = 0.6328 μm. Since the dielectric film is smooth, most energy goes to the specular direction thus a sensitive photomultiplier is used.

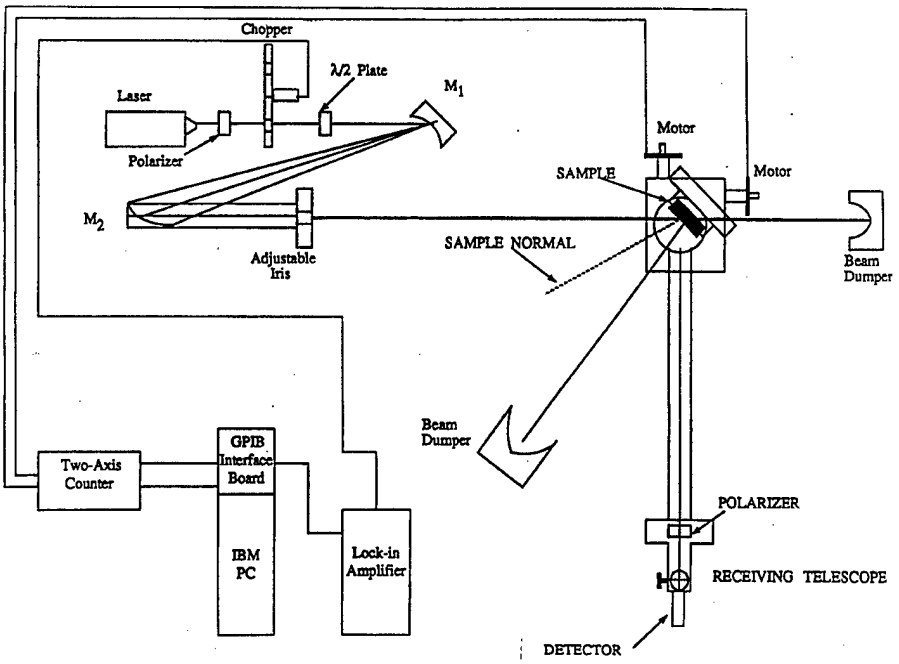

Figure 3. **Schematic of the bidirectional reflectometer.**

In the experiment, the beam size is set to W = 1.5 mm. Since the beam size is small, thus the average far-field speckle size is large. We have to average about 100 measurements to obtain the far-field scattering at each angle by scanning very small yaw and pitch directions of the sample.

Figure 4 (a) shows the experimental results for p-polarization, and Figure 4 (b) for s-polarization with $\theta_i = -89°$. There is a large enhanced backscattering peak at near grazing angle $\theta_s = 89°$. The ratio of backscattering enhancement peak over the surrounding background at $\theta_s = 89°$ for p-polarization is about 19.6 and the ratio of backscattering enhancement peak over the surrounding background at $\theta_s = 89°$ for s-polarization is about 20.4. However in the experiment, the backscattering peak has a finite width and considerable uncertainty appears in determining the peak excess over the surrounding background.

The dependence of K_{0ss} on the angle of incidence θ_i is calculated for layer parameters, corresponding the experiment described above, and shown in figure 5. It is seen that for very low grazing angle $\pi/2 - \theta_i$, the backscattering contrast K_{0ss} can achieve values of several thousands. The plot of $\gamma(\theta_i)$ presented in Figure 6 shows the layer parameters corresponding to the experimental curve in Figure 4b. For $\theta_i = 89^o$, the backscattering peak excess $\gamma \cong 20$, approximately coincides with the value observed in the experiment.

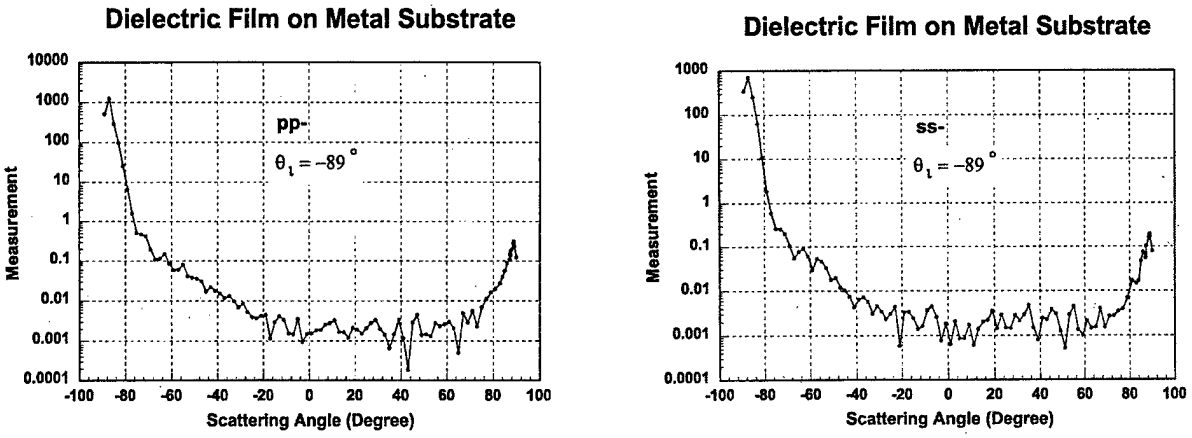

Figure 4. **Experimental results for (a) p-polarization, and (b) for s-polarization.**

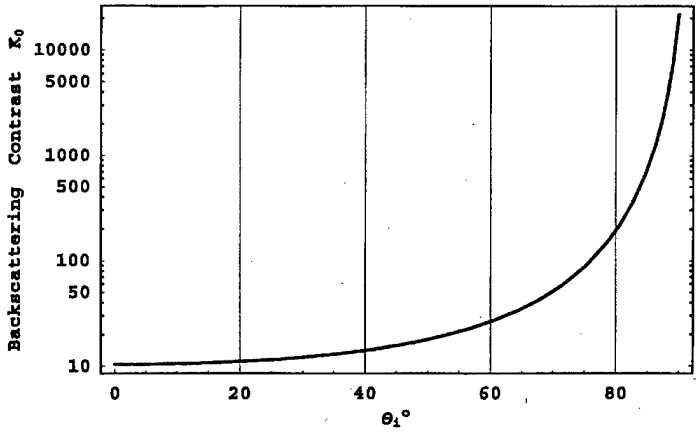

Figure 5. **Backscattering contrast coefficient K_{oss}.**

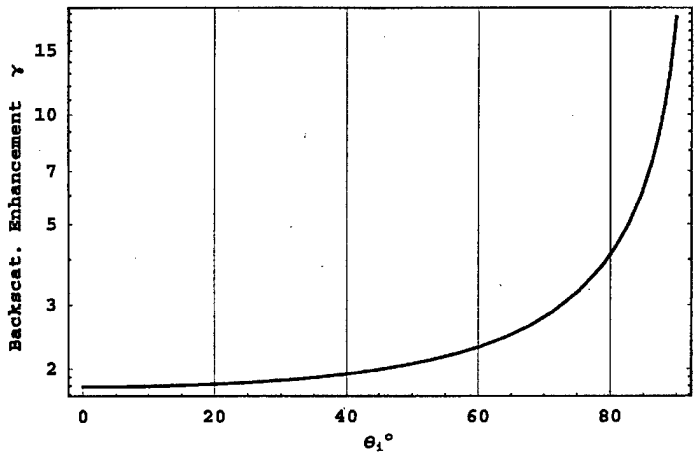

Figure 6. **Backscattering peak enhancement γ.**

4. Summary

In conclusion, backscattering signals at small grazing angle are very important for vehicle re-entrance and lidar signature applications. For a randomly weak rough dielectric film on a reflecting metal substrate, a much larger enhanced backscattering at $\theta_s = 89°$ is measured which is compared with a theoretical calculation. Due to Quetelet's rings, the energy of diffusion is redistributed and a large portion of energy is attracted to the retro-reflection direction at grazing angle. That is why a large backscattering peak appears on the grazing angle.

Acknowledgements

The authors wish to express their gratitude to the U.S. Army Research Office for the support under Grants DAAD19-02-C-0056 and DAAD 19-02-1-0256.

References

1. Sir Isaac Newton, *Optics* (originally published in London, 1704; new edition by Dover, New York, 1952), pp. 289 ff.

2. T. Young, "The Bakerian Lecture: On the theory of light and colors", Philos, Trans. R. Soc. London Part I, 12-48 (1802).

3. P. Selenyi, "Uber Lichtzerstreuung im Raume Wienerscher Interferenzen und neue, diesen reziproke interferenzerscheinungen", Ann. Phys. Chem. 35, 440-460 (1911).

4. Zu-Han Gu, M. Josse, and M. Ciftan, "Observation of Giant Enhanced Backscattering of Light from Weakly Rough Dielectric Films on Reflecting Metal Substrates", Opt. Eng. **35** (2), 370-375 (1996).

5. J.Q. Lu, J.A. Sanchez-Gil, E. Mendez, Zu-Han Gu, and A.A. Maradudin, "Scattering of Light from a Rough Dielectric Film on a Reflecting Substrate: Diffuse Fringes", J. Opt. Soc. Am. A, Vol. **15**, No. 1, 185-195 (1998).

6. Zu-Han Gu, I.M. Fuks, and Mikael Ciftan, "Enhanced Backscattering at Grazing Angles", Optics Letters Vol. **127**, No. 23, 2067-2069 (2002).

7. I.M. Fuks and V.G. Voronovich, "Wave diffraction by rough interfaces in an arbitrary plane-layered medium," Waves Random Media, **10**, 253-272 (2000).

8. I.M. Fuks, "Wave Diffraction by a Rough Boundary of an Arbitrary Plane-Layered Medium", *IEEE Trans. Antennas Propagat.*, **AP-49**, No. 4, pp. 630-639 (2001).

9. A.J. de Witte, "Interference in Scattered Light," Am. J. Phys. **35**, 301-313 (1967).

10. Yu. S. Kaganovskii, V.D. Freilikher, E. Kanzieper, Y. Nafcha, and I.M. Fuks, "Light scattering from slightly rough dielectric films," Opt. Soc. Am. A. **16** (1999).

11. A.I. Kalmykov, V.N. Tcymbal, I.M. Fuks, et al., "Radar observation of strong subsurface scatterers. Model of subsurface reflections," (in Russian), Preprint No. 93-6, Inst. Radiophys. And Electron. Nat. Acad. Sci. Ukraine, Kharkov (1993), English transl. in Telecommunications and Radio Engineering, **52**, 1-17 (1998).